

# Periodic Error Correction in Heterodyne Interferometry

Tony L. Schmitz, Vasishta Ganguly, Janet Yun, and Russell Loughridge

**Abstract** This paper describes periodic error in differential-path interferometry using a Frequency-Path model of the propagation of light from the source to detector in differential-path interferometers. The model identifies each possible path for each light frequency from the source to detector and predicts the number of interference terms that may be expected at the detector output. The behavior of all possible interference terms with respect to optical path changes may be grouped into one of four categories: *Optical Power*, *AC Interference*, *AC Reference*, and *DC Interference*. A description of a single pass, Michelson-type heterodyne interferometer is given and the periodic error is calculated for a selected system.

## I. INTRODUCTION

Differential-path interferometry is used extensively in situations requiring accurate displacement measurements. Commercially available configurations for differential-path interferometers include, but are not limited to, single frequency homodyne and dual frequency heterodyne Michelson-type interferometers with single, double, or multiple passes of the optical paths. Typical applications for these measurement systems are lithographic stages for semiconductor fabrication, transducer calibration, and precision cutting and measuring machines.

Regardless of the optical configuration, all differential-path interferometers infer changes in displacement of a selected optical path by monitoring the optically-induced changes in a photodetector current. The phase-measuring electronics converts this photodetector current to displacement by an assumed relationship between corresponding changes in detector current and displacement, where this assumed relationship is defined by some idealized performance of the optical elements. In reality, the system optics do not behave perfectly and small deviations in the optical signal are induced. Because the final displacement is calculated according to an assumed algorithm in the system electronics, the measurement signal does not exactly reproduce the target motion and errors are generated. In this paper, we describe the physical sources for periodic error.

## II. BACKGROUND

In the literature, investigations of periodic error have generally focused on heterodyne Michelson-type interferometers. In heterodyne systems, imperfect separation of the two light frequencies into the measurement and

reference paths has been shown to produce first and second-order periodic errors, or errors of one and two cycles per wavelength of optical path change, respectively. The two heterodyne frequencies are typically carried on collinear, mutually orthogonal, linearly polarized laser beams in a method referred to as polarization-coding; unwanted leakage of the reference frequency into the measurement path and vice versa may occur due to non-orthogonality between the ideally linear beam polarizations, elliptical polarization of the individual beams, imperfect optical components, parasitic reflections from individual optical surfaces, and/or mechanical misalignment between the interferometer elements (laser, polarizing optics, and targets). In a perfect system, a single wavelength would travel to a fixed reference target, while a second, single wavelength traveled to a moving target. Interference of the combined signals would yield a perfectly sinusoidal trace with phase that varied, relative to a reference phase signal, in response to motion of the moving target. However, the inherent frequency leakage in actual implementations produces an interference signal which is not purely sinusoidal (i.e., contains spurious spectral content) and leads to a periodic, or non-cumulative, error in the measured displacement. Fedotova [1], Quenelle [2], and Sutton [3] performed early investigations of periodic error in heterodyne Michelson interferometers.

## III. FREQUENCY-PATH MODEL

The Frequency-Path (F-P) model is comprised of three fundamental components: the light source composed of one or more frequencies, the detector, which serves as a bridge between the interferometer optics and electronics, and the collection of all available paths between the source and detector consistent with the propagation laws of physical optics [4]. In an ideal interferometer, each source frequency could reach the detector by the intended path only and no frequency leakage would occur between paths. However, due to deviations from the ideal, each frequency may in fact reach the detector by other available paths and contribute to the total electric field. The sum of these individual electric field contributions, or Frequency-Path elements, is then ideally squared at the photodetector, in the absence of saturation, to produce the output current.

A schematic representation of the general F-P model is shown in Figure 1. In the figure, the number of source frequencies is represented by an appropriate number of solid circles in the left column. Similarly, the number of paths from the source to detector, including intentional or unintentional multiple passes, is represented by solid circles in the middle column, while the detector is shown on the right. Each continuous line that connects a given source frequency to the detector through one of the available paths identifies an F-P element (note that these lines do not represent actual optical paths, but rather the electric field contribution from light of a particular frequency, identified in

T.L. Schmitz is an associate professor at the University of North Carolina at Charlotte, Charlotte, NC 28223 USA (phone: 704-687-5086; e-mail: tony.schmitz@uncc.edu).

V. Ganguly is a PhD student at the University of North Carolina at Charlotte, Charlotte, NC 28223 USA (e-mail: vganguly@uncc.edu).

J. Yun is with Agilent Technologies, Santa Clara, CA 95051 USA (e-mail: janet\_yun@agilent.com).

R. Loughridge is with Agilent Technologies, Santa Clara, CA 95051 USA (e-mail: danny@agilent.com).

the left column, reaching the detector via a path identified in the middle column). Furthermore, each of these F-P elements corresponds to an actual light beam in the physical system traveling independently of any other from the source to the detector where the interference takes place.

In the F-P model notation, the electric field amplitude of each F-P element is designated by the letter E appended with two subscripts. The first subscript denotes the source frequency, while the second lists the path from the source to detector. For example,  $E_{21}$ , displayed as a heavy solid line in Figure 1, gives the electric field amplitude of frequency 2 that reaches the detector via path 1.

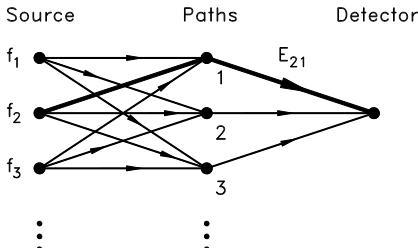


Figure 1. Frequency-Path model – some amount of light (possibly zero) from each source frequency (solid circles in left column) can reach the detector (solid circle on right) by each available path (solid circles in middle column). Each Frequency-Path element is identified by the continuous line connecting a particular source frequency to the detector by one of the available paths.

The squaring action of the photodetector creates  $n(n+1)/2$  distinct interference terms from the sum of  $n$  active F-P elements. In a fully leaking interferometer, for example,  $n$  is equal to the product of the number of frequencies and paths. Each of the interference terms is a product of two F-P elements and it is the superposition of these multiple interference terms in the photodetector current that is converted to displacement by the system electronics. This would appear to generate a complex picture of the photodetector current frequency content. However, these interference terms may be grouped by optical path change dependency into only four categories.

#### A. Equal Frequency Subscripts/Equal Path Subscripts

If the frequency and path subscripts of the two F-P elements of an interference term are both equal, then it corresponds to energy from the same source frequency reaching the detector via the same path, e.g.,  $E_{21}E_{21}$ . This type of interference term is called an Optical Power term and contributes a constant intensity to the photodetector current, independent of optical path changes. There are  $n$  terms of this type, one corresponding to each active F-P element. A particular Optical Power term may in principle, and sometimes in practice, be isolated in the detector by blocking all paths and extinguishing all frequencies, except the frequency and path of interest.

#### B. Unequal Frequency Subscripts/Equal Path Subscripts

This type of interference term corresponds to energy from different source frequencies reaching the detector by the same path, e.g.,  $E_{21}E_{11}$ . It produces a time-harmonic contribution to the photodetector current with a frequency equal to the difference in the optical frequencies of the mode pair involved. Terms of this type are called *AC Reference*

terms with phase that varies by one full cycle over the synthetic wavelength, or the distance defined by the difference in wave numbers ( $\lambda^{-1}$ ) between the source frequencies in question, i.e.,  $\lambda_2^{-1} - \lambda_1^{-1}$  for  $E_{21}E_{11}$ . *AC Reference* terms can be isolated in the detector current by blocking all paths but the one of interest. They may then be observed at the frequency  $f_1 - f_2$ , in this case, using a spectrum analyzer or scope.

#### C. Equal Frequency Subscripts/Unequal Path Subscripts

A *DC Interference* term is produced when energy from one source frequency reaches the detector by two different paths, e.g.,  $E_{21}E_{22}$ . When the optical path is not changing, *DC Interference* terms contribute a DC level to the detector current. This contribution becomes harmonic in time, due to the Doppler effect, when the optical path changes at a constant speed. A specific *DC Interference* term may be observed with a spectrum analyzer by first suppressing all other source frequencies and then noting the signal that is Doppler-shifted from zero frequency during constant velocity target motion. There is also a spatial interference between every pair of *DC Interference* terms, which is again periodic over a distance corresponding to one synthetic wavelength of the two source frequencies involved.

#### D. Unequal Frequency Subscripts/Unequal Path Subscripts

This type of interference term is established when energy from one source frequency reaches the detector by one path, while energy from a second frequency reaches the detector via another path, e.g.,  $E_{21}E_{12}$ . When the target is at rest, *AC Interference* terms produce a time harmonic variation in the detector current at the difference frequency (alternately referred to as the split, reference, or beat frequency) of the modes involved. During target motion, the *AC Interference* term is Doppler-shifted either up or down from the beat frequency, depending on the direction of travel, thus enabling their visual isolation with the aid of a spectrum analyzer.

### IV. F-P MODEL EXAMPLE

As an example of the F-P model, consider a heterodyne, Michelson-type, single pass interferometer. In the ideal case, there are two source frequencies,  $f_1$  and  $f_2$ , and only one possible path for each frequency from the source to the detector, i.e., two F-P elements. One F-P element represents the propagation of the first frequency along its intended path to the reference target, while the other F-P element represents the propagation of the second frequency along its intended path to the moving target. The two F-P elements give a total of  $(2)(2+1)/2 = 3$  interference terms: two *Optical Power* terms and the desired *AC Interference* term. In reality, there are two source frequencies and two possible paths for each frequency from the source to detector (assuming multiple extraneous reflections are neglected) due to imperfect frequency separation at the polarizing beam splitter. In other words, both frequencies can travel to either the reference or moving target in a fully leaking system. This gives four F-P elements and ten distinct interference terms. Figure 2 shows:

a) the F-P model for a heterodyne, Michelson-type, single pass interferometer, b) the actual optical configuration for this interferometer, and c) the four F-P elements as identified from the actual optical configuration.

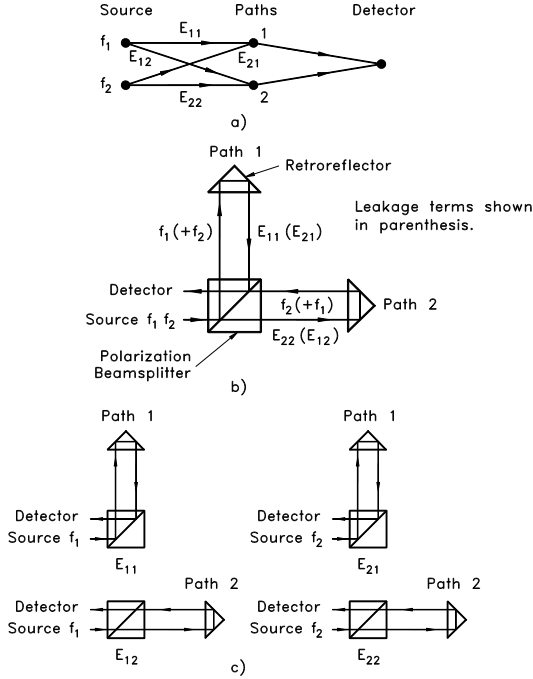


Figure 2. Heterodyne Michelson-type interferometer: a) F-P model with four F-P elements for this configuration; b) physical representation of optics showing F-P elements; and c) identification of physical origin of each F-P element.

Path 1, which ideally contains light of frequency  $f_1$  (expressed in Hz) only (F-P element  $E_{11}$ ) propagates two signals due to frequency leakage:

$$E_{11} \cos(\omega_1 t - k_1 x_1 + \varphi_{11}) \text{ and } E_{21} \cos(\omega_2 t - k_2 x_1 + \varphi_{21}), \quad (1)$$

where the  $\varphi_{ij}$  are the initial phases of the corresponding signals ( $E_{ij}$ ),  $x_1$  represents motion of the target in path 1,  $k_1$  and  $k_2$  are the propagation constants (equal to  $2\pi/\lambda_1$  and  $2\pi/\lambda_2$ , respectively), and  $\omega_{1,2} = 2\pi f_{1,2}$  (rad/s). Similarly, path 2, ideally composed of frequency  $f_2$  light only (F-P element  $E_{22}$ ), also contains two signals:

$$E_{22} \cos(\omega_2 t - k_2 x_2 + \varphi_{22}) \text{ and } E_{12} \cos(\omega_1 t - k_1 x_2 + \varphi_{12}), \quad (2)$$

where the parameter definitions are analogous. The photodetector current is obtained by squaring the sum of the four F-P element electric fields, consisting of two intended and two leakage-induced signals, as shown in (3).

$$\begin{aligned} I \propto E^2 &= \left( E_{11} \cos(\omega_1 t - k_1 x_1 + \varphi_{11}) + E_{21} \cos(\omega_2 t - k_2 x_1 + \varphi_{21}) \right. \\ &\quad \left. + E_{22} \cos(\omega_2 t - k_2 x_2 + \varphi_{22}) + E_{12} \cos(\omega_1 t - k_1 x_2 + \varphi_{12}) \right)^2 \quad (3) \\ &= \frac{E_{11}^2}{2} [\cos(2\omega_1 t - 2k_1 x_1 + 2\varphi_{11}) + 1] + \frac{E_{21}^2}{2} [\cos(2\omega_2 t - 2k_2 x_1 + 2\varphi_{21}) + 1] \\ &\quad + \frac{E_{22}^2}{2} [\cos(2\omega_2 t - 2k_2 x_2 + 2\varphi_{22}) + 1] + \frac{E_{12}^2}{2} [\cos(2\omega_1 t - 2k_1 x_2 + 2\varphi_{12}) + 1] \\ &\quad + E_{22} E_{11} [\cos(\omega_2 t + \omega_1 t - k_2 x_2 - k_1 x_1 + \varphi_{22} + \varphi_{11}) + \cos(\Delta\omega t - k_2 x_2 + k_1 x_1 + \varphi_{22} - \varphi_{11})] \end{aligned}$$

$$\begin{aligned} &+ E_{21} E_{12} [\cos(\omega_2 t + \omega_1 t - k_1 x_2 - k_2 x_1 + \varphi_{21} + \varphi_{12}) + \cos(\Delta\omega t + k_1 x_2 - k_2 x_1 + \varphi_{21} - \varphi_{12})] \\ &+ E_{22} E_{12} [\cos(\omega_2 t + \omega_1 t - k_2 x_2 - k_1 x_1 + \varphi_{22} + \varphi_{12}) + \cos(\Delta\omega t - k_2 x_2 + k_1 x_1 + \varphi_{22} - \varphi_{12})] \\ &+ E_{21} E_{11} [\cos(\omega_2 t + \omega_1 t - k_2 x_1 - k_1 x_1 + \varphi_{21} + \varphi_{11}) + \cos(\Delta\omega t - k_2 x_1 + k_1 x_1 + \varphi_{21} - \varphi_{11})] \\ &+ E_{11} E_{12} [\cos(2\omega_1 t - k_1 x_2 - k_1 x_1 + \varphi_{11} + \varphi_{12}) + \cos(k_1 x_2 - k_1 x_1 + \varphi_{11} - \varphi_{12})] \\ &+ E_{21} E_{22} [\cos(2\omega_2 t - k_2 x_2 - k_2 x_1 + \varphi_{21} + \varphi_{22}) + \cos(k_2 x_2 - k_2 x_1 + \varphi_{21} - \varphi_{22})] \end{aligned}$$

where  $\Delta\omega = \omega_2 - \omega_1$ , and  $\omega_{1,2} = 2\pi f_{1,2}$ .

Equation (3) gives a generic expression for the detector current in the case of a four F-P element system. For the interferometer considered here, we may apply several simplifications to this equation. First, path 1 may be arbitrarily designated as the reference leg and path 2 as the measurement leg. Therefore,  $x_1$  is ideally constant and may be set equal to zero. Second, for a relatively small split frequency between the two heterodyne signals (typically 20 MHz or less in commercially available systems), the propagation constants,  $k_1$  and  $k_2$ , are nearly equal and a single value,  $k$ , may be substituted for each. Third, we may neglect the initial phase of the signals. Finally, due to limited detector bandwidth, those terms which oscillate at twice the optical frequency, or terms which contain  $2\omega_1 t$ ,  $2\omega_2 t$ , or  $\omega_1 t + \omega_2 t$ , may be ignored. After the application of these simplifications, the detector current may be rewritten as the sum of the four types of interference terms described previously; see (4).

$$I \propto E^2 = \left( \frac{E_{11}^2}{2} + \frac{E_{21}^2}{2} + \frac{E_{22}^2}{2} + \frac{E_{12}^2}{2} \right) \text{ Optical Power} \quad (4)$$

$$\begin{aligned} &+ E_{22} E_{11} \cos(\Delta\omega t - kx_2) \text{ AC Interference (intended)} \\ &+ E_{21} E_{12} \cos(\Delta\omega t + kx_2) \text{ AC Interference (leakage-induced)} \\ &+ E_{22} E_{12} \cos(\Delta\omega t) \text{ AC Reference (path 1)} \\ &+ E_{21} E_{11} \cos(\Delta\omega t) \text{ AC Reference (path 2)} \\ &+ E_{11} E_{12} \cos(kx_2) \text{ DC Interference (frequency 1)} \\ &+ E_{21} E_{22} \cos(kx_2) \text{ DC Interference (frequency 2)} \end{aligned}$$

Equation (4) lists all 10 distinct interference terms present in a fully leaking two frequency interferometer. The intended *AC Interference* term is defined by the interference of the  $E_{22}$  and  $E_{11}$  terms, as expected (see Figure 3a). It represents the signal of choice in commercial heterodyne systems. A second *AC Interference* term is obtained due to interference between the leakage terms  $E_{21}$  and  $E_{12}$ , as shown in Figure 3b. This term, generally referred to as the spatial second-harmonic nonlinearity in the literature [5], carries a Doppler phase shift, due to target motion, of equal amplitude, but opposite sign relative to the intended AC term.

The *AC Reference* terms, also referred to as first-harmonic nonlinearities in the literature [5], occur due to interference between the *intended and leakage terms of different frequencies that exist in a single path* of the interferometer (Figures 3c and 3d). As noted previously, these terms exhibit

one full cycle of phase shift over a distance defined by the synthetic wavelength ( $1/\lambda_2 - 1/\lambda_1$ ). For a 20 MHz split frequency, for example, the required displacement is approximately 7.5 m for a single pass interferometer with a fold factor of two.

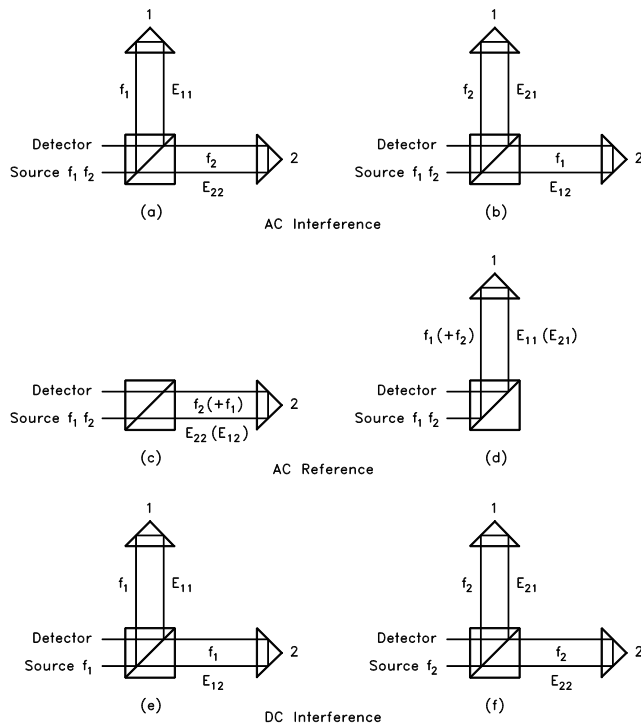


Figure 3. Physical representation of single pass, Michelson-type heterodyne interferometer showing combinations of F-P elements that lead to *AC Interference*, a) and b), *AC Reference*, c) and d), and *DC Interference*, e) and f), terms (*Optical Power* terms are not shown).

Two *DC Interference* terms also exist because *each source frequency is found in each path* (see Figures 3e and 3f). For a commercial single frequency, or homodyne, system, the corresponding *DC Interference* term is the selected measurement signal ( $E_{11}E_{12}$  for frequency  $f_1$ ). These terms exhibit a positive Doppler phase shift of equal amplitude to the *AC Interference* terms regardless of target motion direction, but do not include the  $\Delta\omega t$  phase offset seen in the *AC Interference* terms, i.e., zero frequency shift when the moving target is at rest. Also, in an analogous manner to the *AC Reference* terms, the *DC interference* terms interfere with one another over the synthetic wavelength.

Finally, the *Optical Power* terms are considered. They contribute a DC, or zero frequency, offset to the photodetector current regardless of optical path changes. In general, they do not appear near the intended *AC Interference* term in the frequency domain and, therefore, do not significantly affect the measured displacement. In the case of a homodyne interferometer, however, the intended *DC Interference* term exists within the same passband for low or zero velocity target motion and variations in the *Optical Power* terms cause measurement errors due to the inability of the frequency-selective electronic circuitry to separate the two. This is a fundamental weakness of traditional homodyne interferometers and led to the development of: 1) heterodyne interferometry, and 2) more sophisticated optical configurations for homodyne systems.

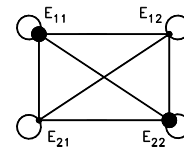


Figure 4. Graphical representation of interference terms resulting from combinations of F-P elements in heterodyne Michelson-type interferometer, where the solid circles signify the F-P elements, horizontal lines denote *DC Interference* terms, vertical lines represent *AC Reference* terms, diagonal lines designate *AC Interference* terms, and loops identify the *Optical Power* terms.

Figure 4 shows a graphical representation of the interference terms that result from combinations of the four F-P elements in a heterodyne Michelson-type interferometer. In this figure, the solid circles signify the F-P elements and the diameters of these circles indicate their relative amplitudes, i.e., it is expected that the intended  $E_{11}$  and  $E_{22}$  terms will be larger than the  $E_{12}$  and  $E_{21}$  leakage terms, the horizontal lines denote *DC Interference* terms, the vertical lines represent *AC Reference* terms, and the diagonal lines designate *AC Interference* terms. The *Optical Power* interference terms are represented by loops originating from and terminating at each F-P element since *Optical Power* terms are the product of an F-P element with itself.

## V. SPECTRAL CONTENT

Each of the interference terms may be seen in the frequency spectrum of the detector current. When the measurement path target is at rest, the intended *AC Interference* term, leakage-induced *AC Interference* term, and *AC reference* terms are found at the beat frequency, which is equal to  $\Delta\omega/(2\pi)$ , while the *DC Interference* and *Optical Power* terms are located at zero frequency. During a constant velocity target motion as shown in Figure 5, the intended *AC Interference* term is either up or down frequency shifted, depending on the moving target direction, by the scalar amount  $\Delta f_d$ , which is proportional to the target velocity (a  $\Delta f_d$  down-shift in the beat frequency is seen in Figure 5). The leakage-induced *AC Interference* term is shifted by the same amount in the opposite direction (up-shifted by  $\Delta f_d$  in this case). The *AC Reference* terms remain at the original beat frequency, except for the slight phase shift introduced by the periodicity of the interference between the two terms over the synthetic wavelength. The *DC Interference* terms are upshifted from zero by  $\Delta f_d$  and the *Optical Power* terms remain at zero frequency.

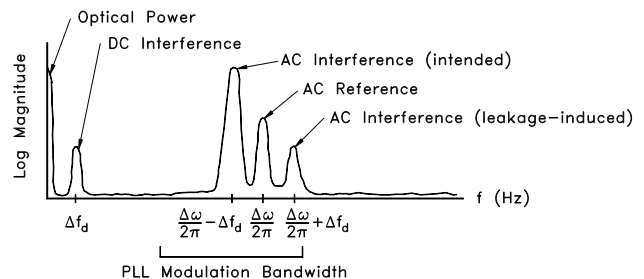


Figure 5. Heterodyne interferometer frequency spectrum for low velocity target motion.

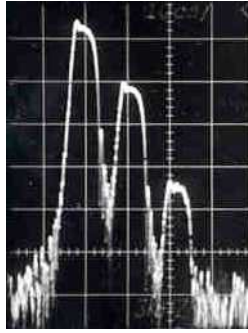


Figure 6. Example spectral content for double pass, Michelson-type heterodyne interferometer.

## VI. PERIODIC ERROR CALCULATION

The relative amplitude of the individual signals and corresponding periodic error is defined by the amount of leakage that occurs due to deviations of the physical realization of the heterodyne interferometer from the ideal. An example calculation of the periodic error for a particular system from spectrum analyzer data is provided here.

Figure 6 displays an example spectrum for a constant (low) velocity displacement measurement using a Michelson-type, double pass heterodyne interferometer. In the figure, the horizontal scale is 5 kHz/division and the vertical scale is 10 dB/division. Additionally, the left peak is the intended *AC Interference* term, the center peak gives the two superimposed *AC Reference* terms (at a beat frequency of 20 MHz), and the right peak is the leakage-induced *AC Interference* term. Due to its larger amplitude, the contribution from the *AC Reference* terms dominates the periodic error in this case. The magnitude of the periodic error,  $\delta x$ , is calculated according to (5), where  $\lambda$  is the source wavelength (633 nm),  $FF$  is the fold factor (= 4 for a double pass configuration), and  $\Delta dB$  is the attenuation of the *AC Reference* signal with respect to the intended *AC Interference* term (14 dB from Figure 6).

$$\delta x = \frac{\lambda}{FF} \left( \frac{10^{\frac{-\Delta dB}{20}}}{2\pi} \right) = \frac{633}{4} \left( \frac{10^{\frac{-14}{20}}}{2\pi} \right) = 5.0 \text{ nm} \quad (5)$$

## VII. CONCLUSION

This paper provided a Frequency-Path model of the propagation of light from the source to detector in differential-path interferometers. This model identifies each possible path for each light frequency from the source to detector and predicts the number of interference terms that may be expected at the detector output. It was shown that, regardless of the interferometer configuration, the behavior of each interference term with respect to optical path changes may be grouped into one of four categories: *Optical Power*, *AC Interference*, *AC Reference*, and *DC Interference*. A description of a single pass, Michelson-type

heterodyne interferometer was provided, but the analysis extends to other cases as well.

## REFERENCES

- [1] G. Fedotova, "Analysis of the measurement error of the parameters of mechanical vibrations," *Measurement Techniques*, vol. 23/7, pp. 577-580, 1980.
- [2] R. Quenelle, "Nonlinearity in interferometric measurements," *Hewlett-Packard Journal*, vol. 34/4, p. 10, 1983.
- [3] C. Sutton, "Nonlinearity in length measurements using heterodyne laser Michelson interferometry," *Journal of Physics E: Scientific Instrumentation*, vol. 20, pp. 1290-1292, 1987.
- [4] T. Schmitz and J. Beckwith, "An investigation of two unexplored periodic error sources in differential-path interferometry," *Precision Engineering*, vol. 27/3, pp. 311-322, 2002.
- [5] V. Badami and S. Patterson, "A frequency domain method for the measurement of nonlinearity in heterodyne interferometry," *Precision Engineering*, vol. 24/1, pp. 41-49, 2000.